Supplemental Material can be found at:
http://www.jbc.org/content/suppl/2012/03/22/M111.325175.DCAuthor_profile.html

THE JOURNAL OF BIOLOGICAL CHEMISTRY VOL. 287, NO. 13, pp. 10265–10275, March 23, 2012
© 2012 by The American Society for Biochemistry and Molecular Biology, Inc. Published in the U.S.A.

# Regulation of *N*-Methyl-D-aspartic Acid (NMDA) Receptors by Metabotropic Glutamate Receptor 7*◆

Received for publication, November 17, 2011, and in revised form, January 24, 2012 Published, JBC Papers in Press, January 27, 2012, DOI 10.1074/jbc.M111.325175

**Zhenglin Gu, Wenhua Liu, Jing Wei, and Zhen Yan**[1]

*From the Department of Physiology and Biophysics, School of Medicine and Biomedical Sciences, State University of New York, Buffalo, New York 14214*

**Background:** The metabotropic glutamate receptors (mGluRs) are potential novel targets for mental disorders.
**Results:** Activation of mGluR7 significantly reduced NMDAR-mediated currents and NMDAR surface expression via an actin-dependent mechanism.
**Conclusion:** mGluR7, by affecting the cofilin/actin signaling, regulates NMDAR trafficking and function.
**Significance:** It provides a potential mechanism for understanding the role of mGluR7 in mental health and disorders.

**Emerging evidence suggests that metabotropic glutamate receptors (mGluRs) are potential novel targets for brain disorders associated with the dysfunction of prefrontal cortex (PFC), a region critical for cognitive and emotional processes. Because *N*-methyl-D-aspartic acid receptor (NMDAR) dysregulation has been strongly associated with the pathophysiology of mental illnesses, we examined the possibility that mGluRs might be involved in modulating PFC functions by targeting postsynaptic NMDARs. We found that application of prototypical group III mGluR agonists significantly reduced NMDAR-mediated synaptic and ionic currents in PFC pyramidal neurons, which was mediated by mGluR7 localized at postsynaptic neurons and involved the β-arrestin/ERK signaling pathway. The mGluR7 modulation of NMDAR currents was prevented by agents perturbing actin dynamics and by the inhibitor of cofilin, a major actin-depolymerizing factor. Consistently, biochemical and immunocytochemical results demonstrated that mGluR7 activation increased cofilin activity and F-actin depolymerization via an ERK-dependent mechanism. Furthermore, mGluR7 reduced the association of NMDARs with the scaffolding protein PSD-95 and the surface level of NMDARs in an actin-dependent manner. These data suggest that mGluR7, by affecting the cofilin/actin signaling, regulates NMDAR trafficking and function. Because ablation of mGluR7 leads to a variety of behavioral symptoms related to PFC dysfunction, such as impaired working memory and reduced anxiety and depression, our results provide a potential mechanism for understanding the role of mGluR7 in mental health and disorders.**

Glutamate, the major excitatory neurotransmitter in prefrontal cortex (PFC),[2] activates both ionotropic and metabotropic glutamate receptors (mGluRs). Preclinical and clinical data suggest that mGluRs, a family of G protein-coupled receptors that comprise eight subtypes (1), are potential novel targets for neuropsychiatric disorders (2–4). Group I mGluR (mGluR1,5) antagonists and group II mGluR (mGluR2,3) agonists are potential anxiolytics (5, 6). Moreover, ligands for group III mGluRs (mGluR4,6,7,8) have anxiolytic- and antidepressant-like effects (7). Among all mGluRs, mGluR7 displays a remarkably low affinity for glutamate and is only activated by millimolar glutamate concentrations, suggesting that it serves as an "emergency" receptor to inhibit glutamatergic transmission under pathophysiological conditions. mGluR7-deficient mice exhibit increased seizure susceptibility (8), impaired working memory (9, 10), deficient fear extinction (11, 12), dysregulated stress responses (13), and reduced anxiety and depression (14, 15).

Previous studies have shown that mGluR7 suppresses voltage-gated $Ca^{2+}$ channels and inhibits synaptic transmission via a presynaptic mechanism depending on PKC and the scaffolding protein PICK1 (16, 17). In the hippocampal mossy fiber pathway, mGluR7 acts as a switch to control the bidirectional plasticity of forward inhibition via compartmentalized $Ca^{2+}$ channel regulation (18, 19). In neocortical regions, mGluR7 mRNA is intensely expressed, whereas the mRNA for other members of group III mGluRs is barely detectable (20, 21). Electron microscopy studies have revealed that mGluR7, in addition to the presynaptic presence, is also postsynaptically distributed in various regions (22–24). Because of the strong effect of mGluR7 on presynaptic glutamate release, the function of mGluR7 at postsynaptic neurons has not been demonstrated in brain slice recordings.

A potential target of postsynaptic mGluR7 that is critical for cognition and emotion is the NMDA glutamate receptor because NMDAR dysregulation has been strongly associated with the pathophysiology of schizophrenia and other mental illnesses (25, 26). Because ablation of mGluR7 leads to a variety of behavioral symptoms related to the abnormality of PFC, a

* This work was supported, in whole or in part, by National Institutes of Health Grants MH84233 and MH85774 (to Z. Y.).
◆ This article was selected as a Paper of the Week.
[1] To whom correspondence should be addressed: Dept. of Physiology and Biophysics, State University of New York, 124 Sherman Hall, Buffalo, NY 14214. E-mail: zhenyan@buffalo.edu.
[2] The abbreviations used are: PFC, prefrontal cortex; mGluR, metabotropic glutamate receptor; mGluRIII, group III mGluR; NMDAR, *N*-methyl-D-aspartic acid receptor; AMPAR, α-amino-3-hydroxy-5-methyl-4-isoxazolepropionic acid receptor; EPSC, excitatory postsynaptic potential; ANOVA, analysis of variance; L-AP4, L-2-amino-4-phosphonobutyrate; L-SOP, L-serine-*O*-phosphate; M-SOP, methylserine-*O*-phosphate; CPPG, (*R*,*S*)-α-cyclopropyl-4-phosphonophenylglycine; cpt-cAMP, 8-(4-chlorophenylthio)-adenosine 3′-5′-monophosphate.

Downloaded from www.jbc.org at State University of NY-Buffalo, on March 29, 2012

brain region critical for cognitive and emotional processes (27–29), we examined the impact of mGluR7 on NMDA receptors in PFC pyramidal neurons. We demonstrate that mGluR7 inhibits NMDAR-mediated currents through a mechanism involving actin-based trafficking of NMDA receptors. It provides a potential molecular and cellular mechanism underlying the involvement of mGluR7 in regulating PFC functions.

## EXPERIMENTAL PROCEDURES

*Electrophysiological Recordings in Slices*—All experiments were carried out with the approval of the State University of New York at Buffalo Animal Care Committee. The voltage clamp recording technique was used to measure NMDAR-EPSC or AMPAR-EPSC in PFC pyramidal neurons as described previously (30, 31). Briefly, PFC brain slices (300 $\mu$m) from juvenile (3–5 weeks postnatal) Sprague-Dawley rat were used. Cells were visualized with a 40× water immersion lens and illuminated with near infrared (IR) light, and the image was detected with an IR-sensitive charge-coupled device (CCD) camera. Tight seals (2–10 gigaohms) from visualized pyramidal neurons were obtained by the "blow and seal" technique. A MultiClamp 700A amplifier was used for these recordings. The access resistances ranged from 13 to 18 megaohms and were compensated 50–70%. A bipolar stimulating electrode (FHC, Inc., Bowdoinham, ME) was positioned ~100 $\mu$m from the neuron under recording. Evoked currents were generated with 50-$\mu$s pulses (delivered every 30 s) from a stimulation isolation unit controlled by an S48 pulse generator (Astro-Med, Inc., West Warwick, RI). For NMDAR-EPSC recording, stimuli were given 3 s after neurons (clamped at −70 mV) were depolarized to +60 mV to fully relieve the voltage-dependent $Mg^{2+}$ block of NMDAR channels.

*Whole-cell Recordings in Dissociated or Cultured Neurons*—Acutely dissociated PFC pyramidal neurons from 4-week-old rats or PFC primary cultures from 17–18-day rat embryos were prepared using procedures described previously (30). Recordings of whole-cell NMDA-elicited currents employed similar techniques as described previously (30, 32). Recordings were obtained with an Axon Instruments 200B patch clamp amplifier that was controlled and monitored with an IBM PC running pCLAMP with a DigiData 1320 series interface. Electrode resistances were typically 2–4 megaohms in the bath. After seal rupture, series resistance (4–10 megaohms) was compensated (70–90%) and periodically monitored. The cell membrane potential was held at −60 mV. NMDA (100 $\mu$M) was applied for 2 s every 30 s to minimize desensitization-induced decrease of current amplitude.

Data analyses were performed with Clampfit (Axon instruments) and KaleidaGraph (Albeck Software, Reading, PA). ANOVA tests were performed to compare the differential degrees of current modulation between groups subjected to different treatments.

*Transfection of Small Interfering RNA*—The small interfering RNA (siRNA) targeting mouse mGluR7 was purchased from Santa Cruz Biotechnology (Santa Cruz, CA). The siRNA against $\beta$-arrestin1 (5′-GGCGAGUCUACGUGACACUtt-3′) and $\beta$-arrestin2 (5′-GGACCGGAASGUGUUUGUGtt-3′) were purchased from Ambion (Austin, TX). Cultured PFC neurons (11 days *in vitro*) were transfected with siRNA using Lipofectamine 2000 (Invitrogen). Cultures were used 2–3 days after transfection.

*Western Blotting*—PFC cultures from 3.5-cm dishes ($1.2 \times 10^6$ cells) were collected and homogenized in 400 $\mu$l of modified radioimmuno precipitation assay buffer (1% Triton X-100, 0.1% SDS, 0.5% deoxycholic acid, 50 mM $NaPO_4$, 150 mM NaCl, 2 mM EDTA, 50 mM NaF, 10 mM sodium pyrophosphate, 1 mM sodium orthovanadate, 1 mM PMSF, and 1 mg/ml leupeptin). Lysates were centrifuged at 4 °C at 16,000 × *g*, and supernatant fractions were collected. After boiling in SDS sample buffer, samples were separated on 15% SDS-PAGE and then transferred to nitrocellulose membranes. Western blotting was carried out using the ECL method according to the manufacturer's protocol (Amersham Biosciences). Antibodies used include: anti-$^{Thr202/Tyr204}$phospho-p44/42 MAP kinase, anti-p44/42 MAP kinase (Cell Signaling, both 1:1000), anti-$^{Ser3}$phospho-cofilin, and anti-cofilin (Cell Signaling, both 1:500).

*Co-immunoprecipitation*—After treatment, PFC slices were homogenized in 1 ml of radioimmune precipitation lysis buffer. The lysates were ultracentrifuged at 100,000 × *g* at 4 °C for 30 min. The supernatant fractions were collected and incubated with anti-NR1 (Millipore, 2 $\mu$g) at 4 °C overnight followed by incubation with protein A/G plus agarose (Santa Cruz Biotechnology) for 2 h. Immunoprecipitates were then subjected to 7.5% SDS-PAGE, transferred to nitrocellulose membranes, and blotted with anti-actin (Santa Cruz Biotechnology, 1:2000) or anti-PSD95 (Affinity BioReagents, 1:2000).

*Immunocytochemical Staining*—Neurons grown on coverslips were fixed in 4% paraformaldehyde in PBS for 20 min at room temperature and then washed three times with PBS. Neurons were then permeabilized with 0.1% Triton X-100 in PBS for 5 min followed by a 1-h incubation with 5% bovine serum albumin (BSA) to block nonspecific staining. For the staining of surface NR1, neurons were fixed but not permeabilized. Neurons were incubated with the primary antibody (anti-MAP2, 1:500, Chemicon; or anti-NR1 extracellular domain, 1:100, Chemicon) at 4 °C overnight. After washing, neurons were incubated with Alexa Fluor 488 (green)-conjugated secondary antibody (Molecular Probes, 1:500) for 2 h at room temperature. For the staining of F-actin, neurons were incubated with Alexa Fluor 568 (red)-conjugated phalloidin (1 unit/ml, Invitrogen) at room temperature for 15 min. After washing in PBS for three times, coverslips were mounted on slides with VECTASHIELD mounting media (Vector Laboratories, Burlingame, CA).

Fluorescent images were obtained using a 100× objective with a cooled charge-coupled device camera mounted on a Nikon microscope. All specimens were imaged under identical conditions and analyzed using identical parameters with the ImageJ software. The surface NR1 clusters or F-actin clusters were measured. To define dendritic clusters, a single threshold was chosen manually so that clusters corresponded to puncta of at least 2-fold greater intensity than the diffuse fluorescence on the dendritic shaft. On each coverslip, the cluster density of 4–6 neurons (3–4 dendritic segments of 50 $\mu$m length per neuron) was measured. Three to four independent experiments for each of the treatments were performed. Quantitative anal-

Downloaded from www.jbc.org at State University of NY-Buffalo, on March 29, 2012

yses were conducted blindly (without knowledge of experimental treatment).

*Biochemical Measurement of Surface NMDA Receptors*—The surface NMDA receptors were detected as described previously (31, 33). Briefly, after treatment, cortical cultures were incubated with artificial cerebrospinal fluid containing 1 mg/ml Sulfo-NHS-LC-Biotin (Pierce Chemical Co.) for 20 min on ice. The cultures were then rinsed three times in TBS to quench the biotin reaction followed by homogenization in 0.5 ml of modified radioimmune precipitation buffer. Lysates were centrifuged at 16,000 × *g* at 4 °C. Supernatant was collected and incubated with NeutrAvidin-agarose (Pierce) for 2 h at 4 °C. Bound proteins were resuspended in SDS sample buffer and boiled. Quantitative Western blots were performed on both total and biotinylated (surface) proteins using anti-NR1 (1:1000; Upstate Biotech Millipore).

## RESULTS

*Activation of mGluR7 Significantly Decreases NMDAR Currents in PFC Pyramidal Neurons*—To examine the potential impact of mGluRs on excitatory synaptic transmission in PFC pyramidal neurons, we examined the effect of L-AP4, a prototypical agonist for group III mGluRs (34, 35), on NMDAR-EPSC and AMPAR-EPSC in PFC slices. As shown in Fig. 1*A*, bath application of L-AP4 (200 μM) caused a strong reversible reduction of the amplitude of NMDAR-EPSC (43.1 ± 6.8%, $n$ = 18). A marked reduction of AMPAR-EPSC by L-AP4 (Fig. 1*B*, 58.3 ± 9.3%, $n$ = 14) was also observed. To distinguish the presynaptic *versus* postsynaptic mechanism underlying these effects of L-AP4, we measured the paired pulse ratio of NMDAR-EPSC and AMPAR-EPSC (evoked by paired pulses with a 100- or 40-ms interval, respectively), a readout sensitive to presynaptic glutamate release. As shown in Fig. 1*C*, L-AP4 did not alter the paired pulse ratio of NMDAR-EPSC (4.9 ± 0.6%, $n$ = 8), but significantly increased the paired pulse ratio of AMPAR-EPSC (37.2 ± 4.2%, $n$ = 8). This suggests that L-AP4 regulates NMDAR-EPSC mainly via a postsynaptic mechanism, whereas regulating AMPAR-EPSC through a presynaptic action.

To verify the postsynaptic effect of L-AP4 on NMDARs, we measured the ionic current elicited by exogenous NMDA application (100 μM) in acutely dissociated PFC pyramidal neurons. As shown in Fig. 1*D*, bath application of L-AP4 (200 μM) reversibly reduced NMDAR currents (24.3 ± 3.6%, $n$ = 12). In contrast, L-AP4 application did not have any significant effect on AMPA (100 μM)-elicited currents (2.6 ± 1.3%, $n$ = 10). To further characterize the effect of L-AP4 on NMDAR currents, we carried out the dose-response experiments. As shown in Fig. 1*E*, L-AP4 started to inhibit NMDAR currents at the dose of 50–100 μM (50 μM: 8.5 ± 2.8%; 100 μM: 16.5 ± 3.1%; $n$ = 8), and reached the saturating level at 200–400 μM (200 μM: 24.3 ± 3.6%; 400 μM: 27.5 ± 4.5%, $n$ = 12), with an $EC_{50}$ ~100 μM.

NMDAR functional properties are determined by subunit composition. The primary NMDARs in mature cortical synapses, which are composed of NR1/NR2A or NR1/NR2B, differ in deactivation kinetics and subcellular distribution. To determine which subpopulation(s) of NMDARs is targeted by L-AP4, we applied the selective inhibitor of NR2B subunit, ifenprodil. Blocking NR2B subunit-containing NMDARs with ifenprodil (10 μM) reduced the amplitude of NMDAR currents by 54.5 ± 2.1% ($n$ = 9). In the presence of ifenprodil, L-AP4 (100 μM) had little effect on the remaining whole-cell NMDAR currents (Fig. 1, *F* and *G*, 2.2 ± 2.4%, $n$ = 9), whereas the reducing effect of L-AP4 was restored after washing off ifenprodil (19.2 ± 1.9%, $n$ = 9). This suggests that L-AP4 primarily targets NR2B subunit-containing NMDA receptors.

To confirm that the effect of L-AP4 on NMDAR currents was mediated through group III mGluRs, we applied selective receptor agonists and antagonists. As shown in Fig. 2*A*, in the presence of mGluRIII antagonists CPPG (50 μM) or M-SOP (400 μM), the reducing effect of L-AP4 on NMDAR currents was significantly diminished (CPPG: 5.1 ± 0.8%, $n$ = 8; M-SOP: 6.3 ± 0.9%, $n$ = 8; Fig. 2*B*). Another selective group III mGluR agonist, L-SOP (400 μM), also reduced NMDAR currents (Fig. 2*B*, 20.4 ± 2.8%, $n$ = 10), and the effect of L-SOP was largely blocked by the antagonist CPPG (4.8 ± 0.8%, $n$ = 8) and M-SOP (6.7 ± 1.0%, $n$ = 8).

Using cell lines that express specific mGluR subtypes, it has been determined that neither L-AP4 nor L-SOP possesses activity at group I or II mGluRs at concentrations below 1000 μM, whereas L-AP4 has $EC_{50}$ of 160–500 μM to mGluR7 and 0.4–1.2 μM to other members in group III (mGluR4,6,8) (34, 35). Similarly, L-SOP has $EC_{50}$ of ~200 μM to mGluR7 and 2–5 μM to other members in group III (34, 35). Because of the pharmacological profile of mGluRs, previous physiological studies on the role of group III mGluRs, especially mGluR7, in synaptic transmission have commonly used high doses (500–1000 μM) of L-AP4 (19, 36–38). Our dose-response studies suggest that mGluR7 is the receptor mediating the effect of L-AP4 on NMDAR currents. To confirm this, we carried out a cellular knockdown experiment with mGluR7 siRNA transfection in PFC cultures. As shown in Fig. 2*C*, the reducing effect of L-AP4 on NMDAR currents was abolished in mGluR7 siRNA-transfected neurons (control: 22.3 ± 3.1%, $n$ = 8; mGluR7 siRNA: 5.5 ± 1.1%, $n$ = 6). Taken together, these results suggest that activation of mGluR7 suppresses NMDAR currents via a postsynaptic mechanism in PFC pyramidal neurons.

*β-Arrestin2/ERK Signaling Pathway Is Involved in mGluR7 Regulation of NMDAR Currents*—We then investigated the signaling mechanisms underlying mGluR7 reduction of NMDAR currents. Group III mGluRs are thought to be primarily coupled to $G_{i/o}$ proteins to inhibit cAMP formation and PKA activation (39). Thus, we first tested the involvement of PKA. As shown in Fig. 3, *A* and *C*, the L-AP4 reduction of NMDAR currents in dissociated PFC pyramidal neurons was not significantly changed by either PKA activator cpt-cAMP (21.6 ± 3.8%, $n$ = 8) or PKA inhibitor PKI14–22 (22.2 ± 3.5%, $n$ = 8). Other than the PKA signaling pathway, previous studies have shown that L-AP4 can activate PI3K and ERK pathways in cultured cerebellar granule cells (21). Thus, we tested their potential involvement. As shown in Fig. 3, *B* and *C*, the L-AP4 reduction of NMDAR currents was largely blocked by the ERK kinase inhibitor PD98059 (50 μM, 8.6 ± 2.5%, $n$ = 10) or U0126 (20 μM, 7.1 ± 2.1%, $n$ = 10), but not by the PI3K inhibitor wortmannin (0.5 μM, 17.2 ± 3.3%, $n$ = 8) or LY294002 (100 μM,

Downloaded from www.jbc.org at State University of NY-Buffalo, on March 29, 2012

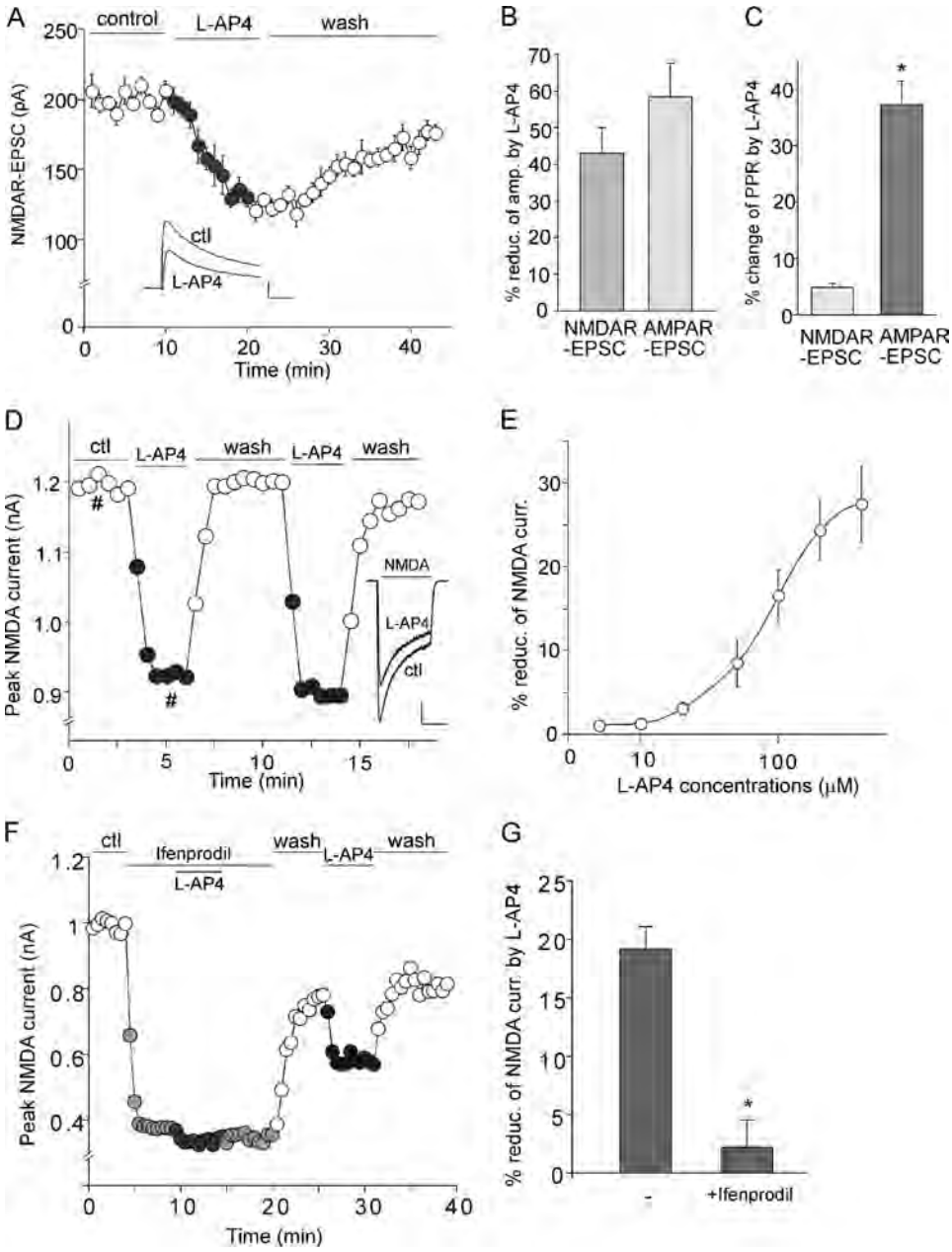


FIGURE 1. **Group III mGluR agonist L-AP4 reversibly reduces NMDAR currents in PFC pyramidal neurons.** *A*, plot of peak NMDAR-EPSC showing the effect of L-AP4 (200 μM) on NMDAR-mediated synaptic responses in PFC slices. *Insets*, representative current traces (average of three trials). *Scale bars*, 50 pA, 50 ms. *ctl*, control. *B*, bar graphs (mean ± S.E.) showing the percentage of reduction of NMDAR-EPSC or AMPAR-EPSC amplitudes by L-AP4. *C*, bar graphs (mean ± S.E.) showing the percentage change of paired pulse ratio (*PPR*) of NMDAR-EPSC or AMPAR-EPSC by L-AP4. *, $p < 0.001$, ANOVA. *D*, plot of peak NMDA-elicited ionic currents as a function of time and L-AP4 (200 μM) application in an acutely dissociated PFC pyramidal neuron. *Inset*, current traces (at time points denoted by #). *Scale bars*, 0.2 nA, 1 s. *E*, dose-response curve showing the percentage reduction of NMDAR currents by different concentrations of L-AP4 in dissociated PFC neurons. *F*, plot of peak NMDAR currents showing the effect of L-AP4 (100 μM) during ifenprodil (10 μM) application and after washing off ifenprodil in a dissociated PFC pyramidal neuron. *G*, bar graphs (mean ± S.E.) summarizing the percentage of reduction of NMDAR currents by L-AP4 in the absence or presence of ifenprodil. *, $p < 0.001$, ANOVA.

17.8 ± 3.5%, $n = 8$). These results suggest that ERK signaling is specifically involved in mGluR7 regulation of NMDAR currents in PFC pyramidal neurons.

We further tested whether group III mGluRs could lead to the activation of ERK (indicated by $Thr^{202}/Tyr^{204}$ phospho-ERK) in PFC. As shown in Fig. 3*D*, L-AP4 treatment (200 μM, 10 min) significantly elevated the level of activated ERK (1.8 ± 0.2-fold increase, $n = 8$) in cultured PFC neurons, and the increase was almost completely blocked by group III mGluR antagonist CPPG (50 μM, 0.2 ± 0.03-fold increase, $n = 6$) or ERK kinase inhibitor PD98059 (50 μM, 0.3 ± 0.04-fold increase, $n = 6$).

Next, we tested what signaling pathway underlies the activation of ERK by L-AP4. It has been shown that some G proteins form a signaling complex with the multifunctional adaptor and transducer molecule, β-arrestin1/2, which recruits and activates components of the MAP kinase cascades (40, 41). Thus, we examined the potential involvement of β-arrestins in L-AP4 activation of ERK and L-AP4 suppression of NMDAR currents. The siRNA against β-arrestin1 or β-arrestin2, which can spe-

Downloaded from www.jbc.org at State University of NY-Buffalo, on March 29, 2012

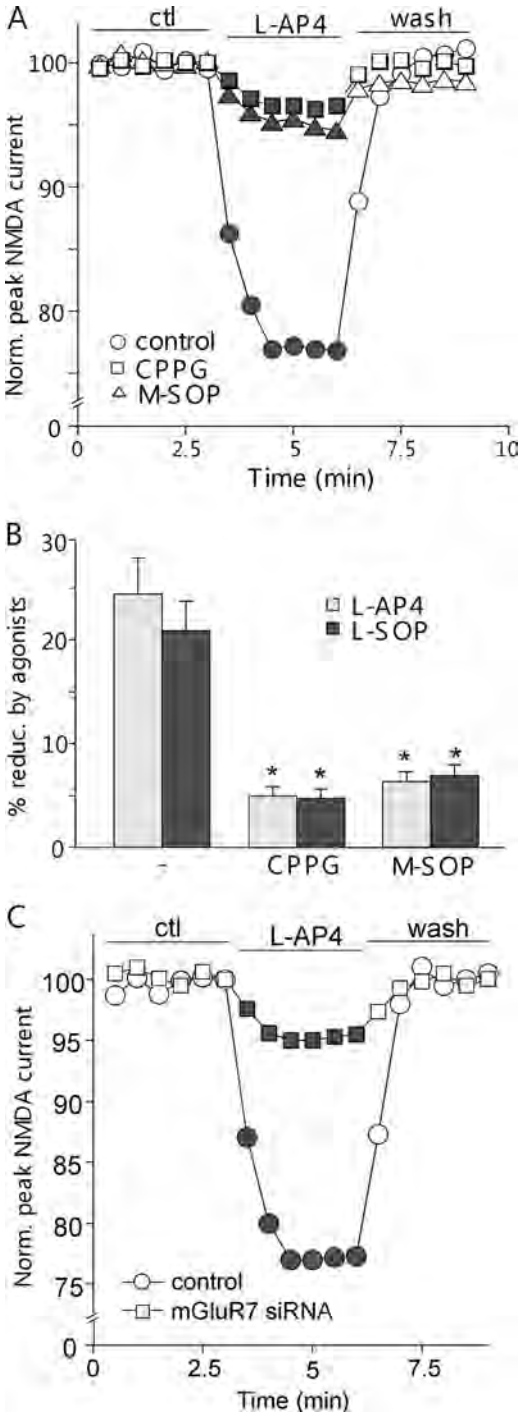


FIGURE 2. **mGluR7 mediates L-AP4 reduction of NMDAR currents.** *A*, plot of normalized (*Norm.*) peak NMDAR currents in dissociated PFC pyramidal neurons showing the effect of L-AP4 (200 $\mu$M) in the absence or presence of group III mGluR antagonists CPPG (50 $\mu$M) or M-SOP (400 $\mu$M). *ctl*, control. *B*, cumulative data (mean ± S.E.) showing the percentage of reduction (*% reduc.*) of NMDAR currents by group III mGluR agonists L-AP4 or L-SOP (400 $\mu$M) in the absence (control) or presence of antagonists CPPG or M-SOP. *, $p < 0.001$, ANOVA, compared to the effects in the absence of the antagonists (−). *C*, plot of normalized peak NMDAR currents showing the effect of L-AP4 (200 $\mu$M) in cultured PFC pyramidal neurons transfected with or without mGluR7 siRNA.

cifically and effectively knock down their protein expression (42), were used to transfect PFC cultures. As shown in Fig. 4, *A* and *B*, the L-AP4-induced reduction of NMDAR currents was markedly attenuated in $\beta$-arrestin2 siRNA-transfected neurons (7.3 ± 0.9%, $n = 10$), but not in $\beta$-arrestin1 siRNA-transfected neurons (21.5 ± 2.6%, $n = 10$). In addition, the L-AP4-induced activation of ERK was largely blocked in $\beta$-arrestin2 siRNA-transfected cultures (Fig. 4*C*, 0.3 ± 0.05-fold increase, $n = 8$). These results suggest that mGluR7 regulates NMDAR currents via activation of $\beta$-arrestin2/ERK signaling.

*mGluR7 Reduction of NMDAR Currents Depends on Mechanism Involving Cofilin-regulated Actin Cytoskeleton*—We next investigated the potential mechanisms underlying mGluR7 regulation of NMDAR currents. After NMDARs leave the endoplasmic reticulum, they are transported first along microtubules on dendritic shafts and then along actin filaments in dendritic spines before being delivered to the synaptic membrane. Our previous studies have shown that neuromodulators could affect NMDAR trafficking via mechanisms depending on the integrity of these cytoskeletal systems (30, 32). Thus, we examined whether L-AP4 reduction of NMDAR currents is through an actin- or microtubule-dependent mechanism. As shown in Fig. 5*A*, pretreatment with the actin-depolymerizing agent latrunculin B (5 $\mu$M, 20 min) prevented the effect of L-AP4 on NMDAR currents (6.9 ± 1.6%; $n = 8$, Fig. 5*C*). Dialysis with the actin stabilizer phalloidin (2 $\mu$M) also blocked the effect of L-AP4 (8.6 ± 1.3%, $n = 9$, Fig. 5*C*). In contrast, the effect of L-AP4 on NMDAR currents was not altered by the microtubule depolymerizer nocodazole (50 $\mu$M, Fig. 5*B*, 20.8 ± 3.8%, $n = 6$, Fig. 5*C*) or the microtubule stabilizer taxol (10 $\mu$M, Fig. 5*B*, 21.9 ± 3.9%, $n = 6$, Fig. 5*C*). It suggests that mGluR7 reduces NMDAR currents by interfering with the trafficking of NMDA receptors along actin filaments.

The dynamics of actin assembly are regulated by several key proteins, one of which is cofilin (43), an important member of the actin-depolymerizing factor (ADF) family. The activity of cofilin is mainly regulated by phosphorylation at a single site ($Ser^3$). Dephosphorylation at this site greatly increases the actin-depolymerizing activity of cofilin (44). Thus, we tested whether mGluR7 might regulate actin-based NMDAR trafficking by interfering with cofilin-mediated actin depolymerization.

First, we examined whether mGluR7 could affect the phosphorylation and activity of cofilin. As shown in Fig. 6, *A* and *B*, with an antibody specifically recognizing $^{Ser3}$phospho-cofilin, L-AP4 treatment (200 $\mu$M, 10 min) significantly decreased the level of $Ser^3$-phosphorylated cofilin in cultured PFC neurons (63 ± 11% of control, $n = 8$), which was prevented by pretreatment with the ERK kinase inhibitor PD98059 (105 ± 19% of control, $n = 6$). This suggests that mGluR7 activation increases the actin-depolymerizing activity of cofilin via an ERK-dependent mechanism. Consistently, the ERK signaling pathway has been shown to mediate cofilin dephosphorylation and activation induced by Src or Ras in non-neuronal cells (45, 46).

Next, we tested whether cofilin was involved in L-AP4 regulation of NMDAR currents. Because cofilin is inactivated by phosphorylation at $Ser^3$ and reactivated by dephosphorylation, two peptides consisting of 1–16 residues of cofilin with or without $Ser^3$-phosphorylated (47, 48) were used. The phospho-cofilin peptide serves as an inhibitor of endogenous cofilin because it binds to cofilin phosphatases and thus prevents the dephosphorylation (activation) of endogenous cofilin, whereas

Downloaded from www.jbc.org at State University of NY-Buffalo, on March 29, 2012

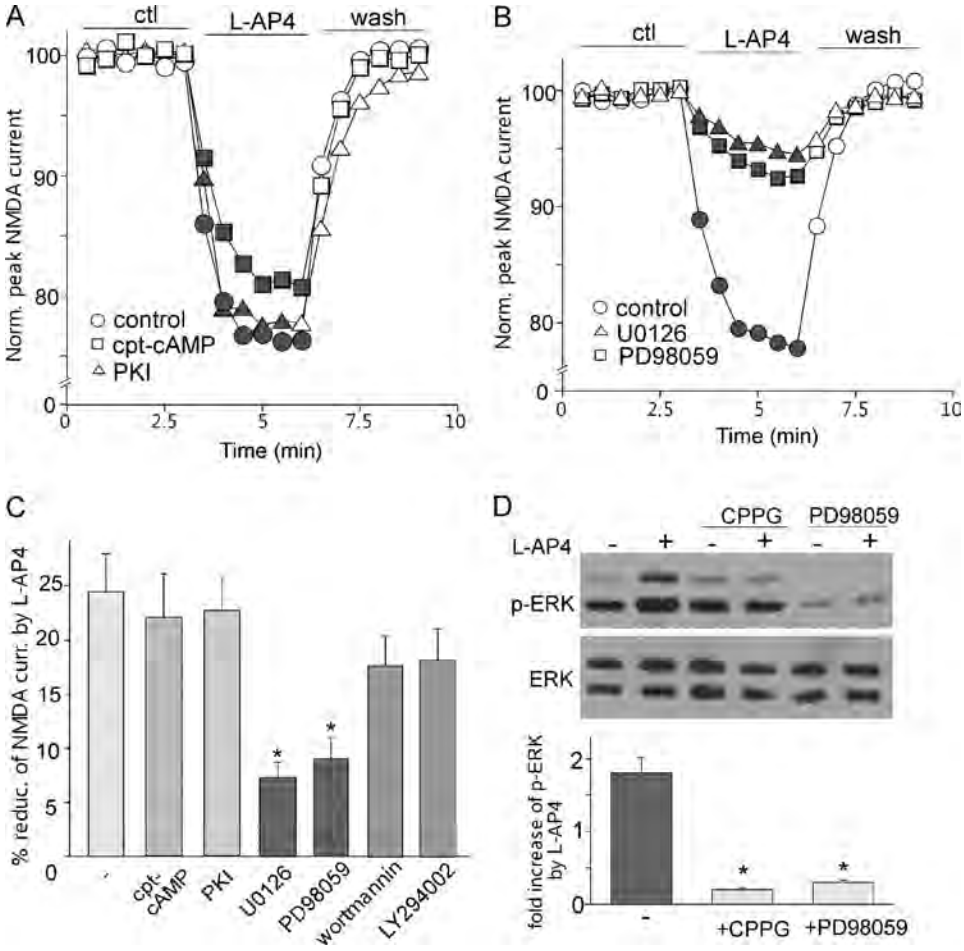


FIGURE 3. **Activation of ERK is required for mGluR7 reduction of NMDAR currents.** *A*, plots of normalized (*Norm.*) peak NMDAR currents in dissociated PFC pyramidal neurons showing the effect of L-AP4 (200 $\mu$M) in the absence or presence of PKA activator cpt-cAMP (100 $\mu$M) or PKA inhibitor PKI14–22 (*PKI*, 0.1 $\mu$M, myristoylated). *ctl*, control. *B*, plots of normalized peak NMDAR currents showing the effect of L-AP4 (200 $\mu$M) in the absence or presence of ERK kinase inhibitors U0126 (20 $\mu$M) or PD98059 (50 $\mu$M). *C*, cumulative data (mean ± S.E.) showing the percentage of reduction (*% reduc.*) of NMDAR currents (*curr.*) by L-AP4 in the presence of cpt-cAMP, PKI14–22, U0126, PD98059, wortmannin (1 $\mu$M), or LY294002 (100 $\mu$M). *, $p < 0.001$, ANOVA. *D*, *top*, Western blotting of phospho-ERK (*p-ERK*) and total ERK in cultured PFC neurons showing the effect of L-AP4 in the absence or presence of CPPG or PD98059. *Bottom*, quantitative analysis showing the -fold increase of phospho-ERK by L-AP4 under different conditions. *, $p < 0.001$, ANOVA.

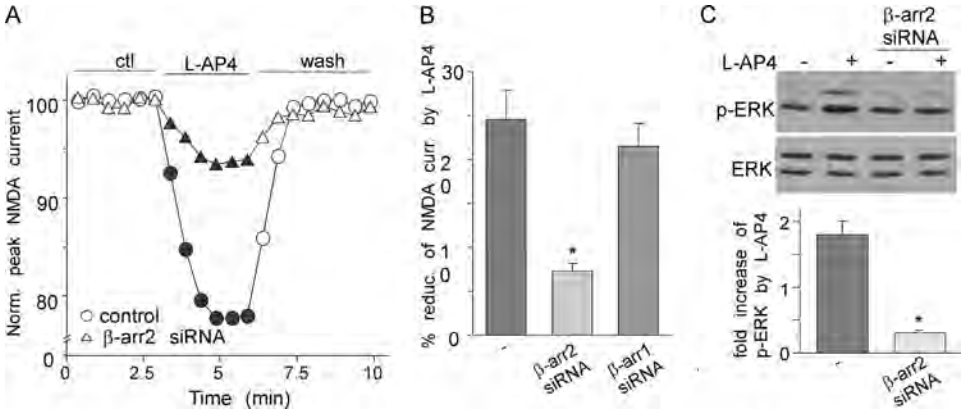


FIGURE 4. ***β*-Arrestin2 is involved in mGluR7 reduction of NMDAR currents and activation of ERK.** *A*, plots of normalized (*Norm.*) peak NMDAR currents showing the effect of L-AP4 in cultured PFC neurons transfected without or with *β*-arrestin2 (*β-arr2*) siRNA. *ctl*, control. *B*, cumulative data (mean ± S.E.) showing the percentage of reduction (*% reduc.*) of NMDAR currents (*curr.*) by L-AP4 in cultures transfected with siRNA against *β*-arrestin1 or *β*-arrestin2. *, $p < 0.001$, ANOVA. *C*, Western blotting analysis showing the effect of L-AP4 on ERK activation (phosphorylation (*p-ERK*)) in cultured PFC neurons transfected without or with *β*-arrestin2 siRNA. *, $p < 0.001$, ANOVA.

the cofilin peptide serves as a negative control. As shown in Fig. 6*C*, the effect of L-AP4 on NMDAR currents was significantly diminished in neurons dialyzed with the phospho-cofilin peptide (100 $\mu$M, 11.3 ± 2.1%, $n = 10$, Fig. 6*D*), as compared with control neurons (24.0 ± 2.8%, $n = 8$), whereas the cofilin peptide (100 $\mu$M) failed to alter the L-AP4 effect (24.5 ± 3.9%, $n = 8$,

Downloaded from www.jbc.org at State University of NY-Buffalo, on March 29, 2012

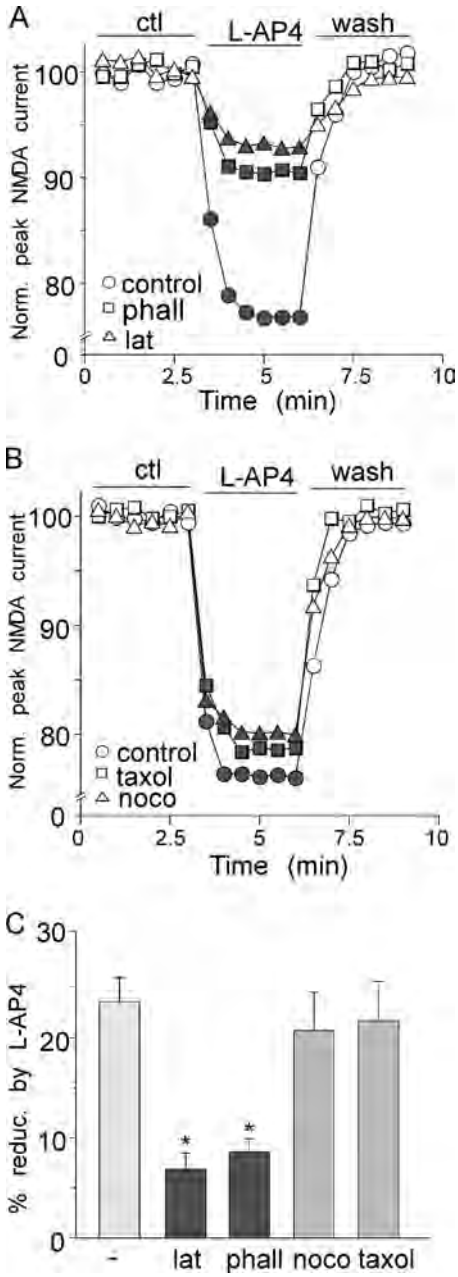


FIGURE 5. **mGluR7 regulates NMDAR currents via actin-dependent mechanism.** *A*, plots of normalized (*Norm.*) peak NMDAR currents showing the effect of L-AP4 in PFC pyramidal neurons treated with actin depolymerizer latrunculin B (*lat*, 5 $\mu$M) or dialyzed with actin stabilizer phalloidin (*phall*, 2 $\mu$M). *ctl*, control. *B*, plots of normalized peak NMDAR currents showing the effect of L-AP4 in PFC pyramidal neurons treated with microtubule depolymerizer nocodazole (*noco*, 40 $\mu$M) or microtubule stabilizer taxol (10 $\mu$M). *C*, cumulative data (mean ± S.E.) showing the percentage of reduction (*% reduc.*)of NMDAR currents by L-AP4 in the absence or presence of various agents affecting actin or microtubule stability. *, $p < 0.001$, ANOVA.

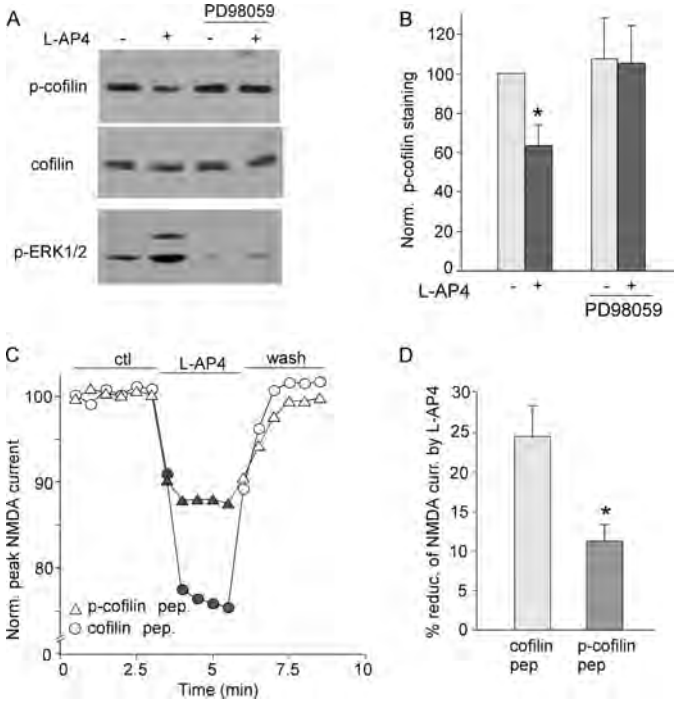


FIGURE 6. **Major actin-depolymerizing factor cofilin is involved in mGluR7 reduction of NMDAR currents.** *A*, Western blotting of Ser[3]-phosphorylated cofilin (*p-cofilin*), total cofilin, and phospho-ERK1/2 (*p-ERK1/2*) in cultured PFC neurons treated without or with L-AP4 (200 $\mu$M, 10 min) in the absence or presence of ERK kinase inhibitor PD98059 (50 $\mu$M, added 15 min prior to L-AP4 application). *B*, cumulative data (mean ± S.E.) showing the effect of L-AP4 on phospho-cofilin under different conditions. *Norm.*, normalized. *C*, plot of normalized peak NMDAR currents showing the L-AP4 effect in cells dialyzed with the phospho-cofilin peptide (*p-cofilin pep.*, 200 $\mu$M) or the cofilin peptide (200 $\mu$M). *D*, cumulative data (mean ± S.E.) showing the percentage of reduction (*% reduc.*) of NMDAR currents (*curr.*) by L-AP4 in neurons loaded with different peptides. *, $p < 0.001$, ANOVA.

Fig. 6*D*). These results suggest that mGluR7 may reduce NMDAR currents by increasing cofilin activity and the ensuing actin depolymerization.

To further confirm the involvement of actin dynamics in mGluR7-induced signaling, we directly examined the effect of L-AP4 on actin depolymerization. Immunocytochemical staining of filamentous actin was performed with rhodamine-phalloidin in cultured PFC neurons. As shown in Fig. 7, *A* and *B*, L-AP4 treatment (200 $\mu$M, 10 min) significantly reduced the density of F-actin clusters (control: 73.7 ± 5.8 clusters/100 $\mu$m; L-AP4: 47.5 ± 3.6 clusters/100 $\mu$m, $n = 30$, $p < 0.001$, ANOVA), and the reduction was largely blocked by PD98059 (PD98059, 78.1 ± 6.1 clusters/100 $\mu$m; PD98059 + L-AP4: 72.6 ± 6.6 clusters/100 $\mu$m, $n = 30$, $p > 0.05$, ANOVA), suggesting that mGluR7 activation induces significant F-actin depolymerization in an ERK-dependent manner.

*Activation of mGluR7 Decreases Surface Level of NMDARs through Actin-dependent Mechanism*—Next, we would like to know how mGluR7-induced actin depolymerization leads to the suppression of NMDAR currents. Previous studies have suggested that the integrity of actin cytoskeleton is important for stabilizing and/or promoting surface NMDAR expression (30, 49), so we tested the involvement of NMDAR trafficking in mGluR7 regulation of NMDAR currents. We first examined whether mGluR7 affects the association of NMDARs with actin cytoskeleton. As shown in Fig. 8, L-AP4 treatment caused a significant decrease of the binding between NR1 and actin (53.0 ± 8.8%, $n = 8$), and this effect was blocked by pretreatment (15 min prior to L-AP4 application) with the mGluRIII antagonist CPPG (8.0 ± 1.3%, $n = 6$) or the membrane-permeable actin stabilizer phalloidin oleate (5.0 ± 1.1%, $n = 6$). Because the clathrin-dependent

Downloaded from www.jbc.org at State University of NY-Buffalo, on March 29, 2012

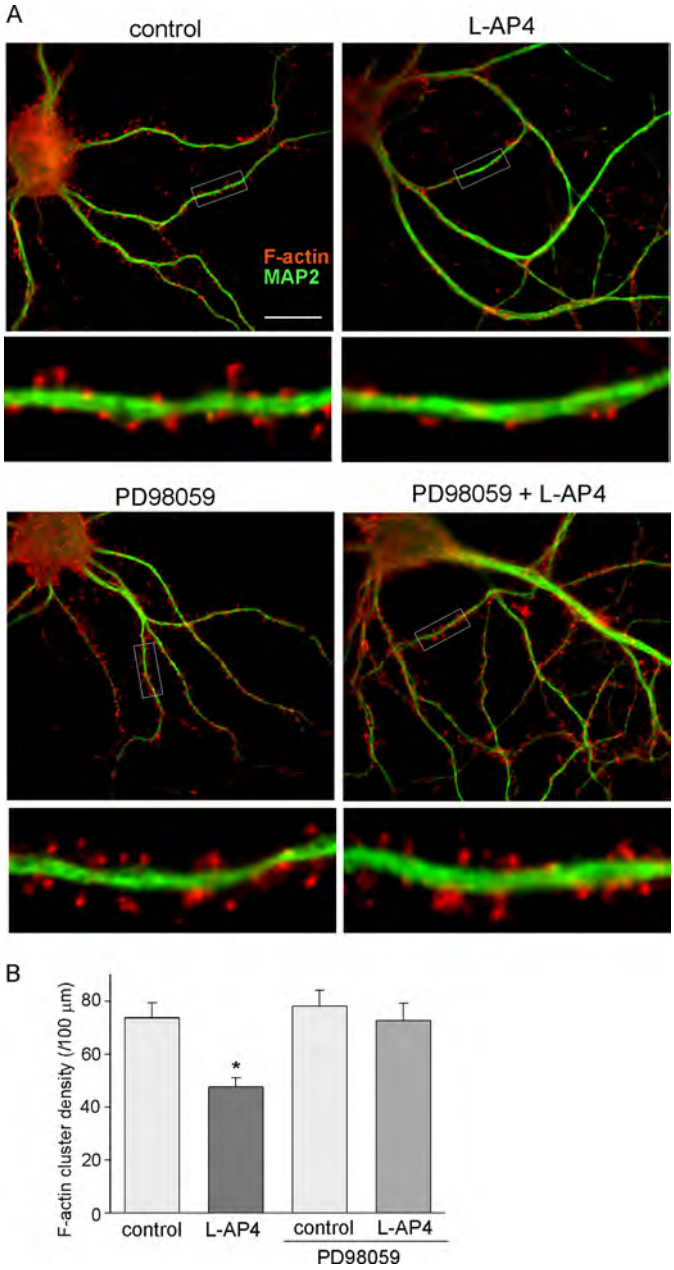


FIGURE 7. **mGluR7 reduces F-actin via ERK-dependent mechanism.** *A*, immunostaining of F-actin (phalloidin, *red*) and MAP2 (*green*) in cultured PFC neurons treated without or with L-AP4 (200 μM, 10 min). Enlarged versions of the *boxed regions* of the dendrites are shown beneath each of the images. *B*, cumulative data (mean ± S.E.) showing the effect of L-AP4 on F-actin cluster density in the absence or presence of PD98059 (50 μM, added 15 min prior to L-AP4 application). *, $p < 0.001$, ANOVA.

internalization of NMDARs is prevented by the postsynaptic scaffolding protein PSD-95 (50, 51), we further tested whether mGluR7 affects the association of NR1 and PSD-95 in an actin-dependent manner. As shown in Fig. 8, L-AP4 treatment significantly decreased the binding between NR1 and PSD-95 (37.0 ± 5.6%, $n = 8$), which was also prevented by CPPG (6.0 ± 1.1%, $n = 6$) or phalloidin oleate (2.0 ± 0.5%, $n = 6$). These data suggest that mGluR7-induced actin depolymerization results in less NR1 binding to actin assembly, which may contribute to the dissociation of NMDARs from the scaffold protein complex.

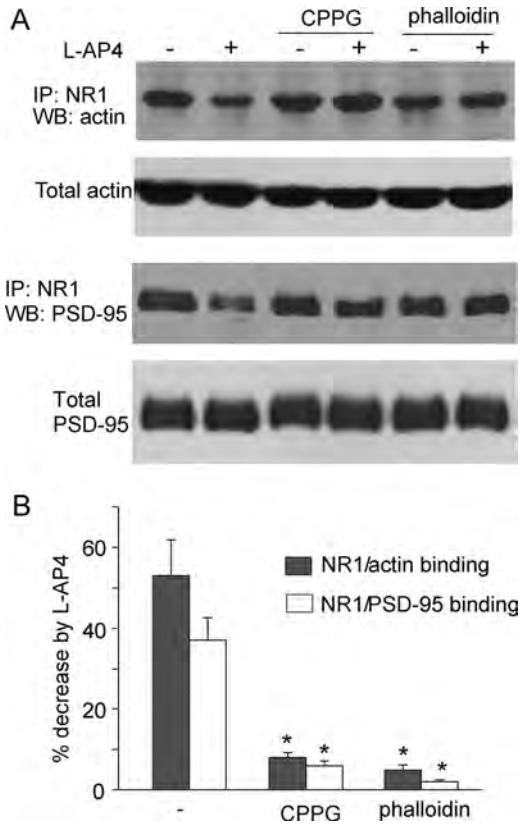


FIGURE 8. **mGluR7 reduces NR1 binding to actin and PSD-95.** *A*, co-immunoprecipitation (*IP*) and Western blot (*WB*) analysis showing the effect of L-AP4 treatment (200 μM, 10 min) on the interaction of NR1 with actin or PSD-95 in the absence or presence of mGluRIII antagonist CPPG (50 μM) or actin stabilizer phalloidin oleate (1 μM). *B*, cumulative data (mean ± S.E.) showing the effect of L-AP4 on NR1-actin binding or NR1-PSD-95 binding under different conditions. *, $p < 0.001$, ANOVA.

The decreased binding between NR1 and PSD-95 in response to L-AP4 could result in reduced surface expression of NMDARs. To test this, we performed immunochemical staining of surface NR1 using an antibody recognizing the extracellular domain of NR1 in cultured PFC neurons under the nonpermeabilized condition. As shown in Fig. 9*A*, L-AP4 treatment significantly decreased the density of surface NR1 clusters (control: 36.8 ± 2.2 clusters/100 μm; L-AP4: 25.4 ± 1.8 clusters/100 μm, $n = 30$, $p < 0.001$, ANOVA), which was prevented by pretreatment with phalloidin oleate (phalloidin: 38.2 ± 2.8 clusters/100 μm; phalloidin + L-AP4: 35.3 ± 2.6 clusters/100 μm, $n = 30$, $p > 0.05$, ANOVA).

To further complement the staining results, we also performed surface biotinylation experiments (31, 33) to measure the level of surface NR1 in PFC slices. Surface proteins were labeled with sulfo-NHS-LC-biotin, and then biotinylated surface proteins were separated from nonlabeled intracellular proteins by reaction with NeutrAvidin beads. Surface and total proteins were subjected to electrophoresis and probed with an antibody against the NR1 subunit. As shown in Fig. 9, *B* and *C*, L-AP4 treatment significantly decreased the level of surface NR1 (28.7 ± 2.1% decrease, $n = 8$), which was blocked by pretreatment with phalloidin oleate (5.5 ± 0.6% decrease, $n = 8$). These results suggest that mGluR7 activation decreases the level of surface NMDARs through an actin-de-

Downloaded from www.jbc.org at State University of NY-Buffalo, on March 29, 2012

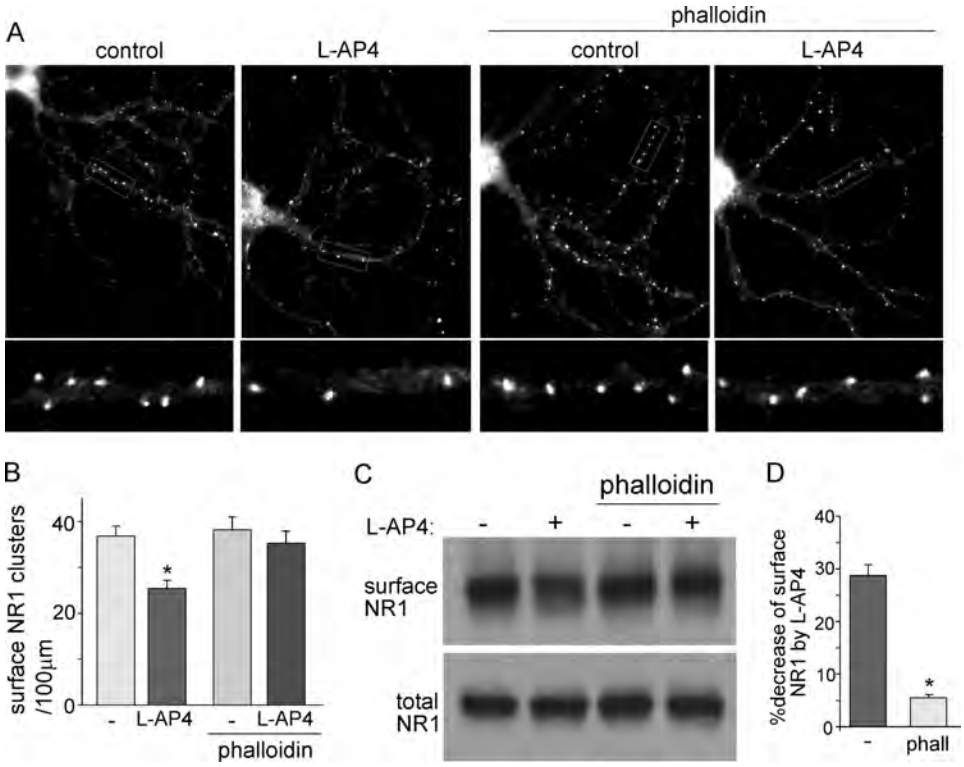


FIGURE 9. **mGluR7 reduces level of surface NMDARs via actin-dependent mechanism.** *A*, immunocytochemical staining of surface NR1 in PFC pyramidal neurons treated without (*control*) or with L-AP4 (200 $\mu$M, 10 min) in the absence or presence of actin stabilizer phalloidin oleate (1 $\mu$M, added 15 min prior to L-AP4 application). *B*, cumulative data (mean ± S.E.) showing the effect of L-AP4 on surface NR1 cluster density under different conditions. *, $p < 0.001$, ANOVA. *C*, Western blotting of surface or total NR1 from cultured PFC neurons treated without or with L-AP4 in the absence or presence of phalloidin oleate. *D*, cumulative data (mean ± S.E.) showing the effect of L-AP4 on the expression level of surface NR1 under different conditions. *, $p < 0.001$, ANOVA. *Phall*, phalloidin.

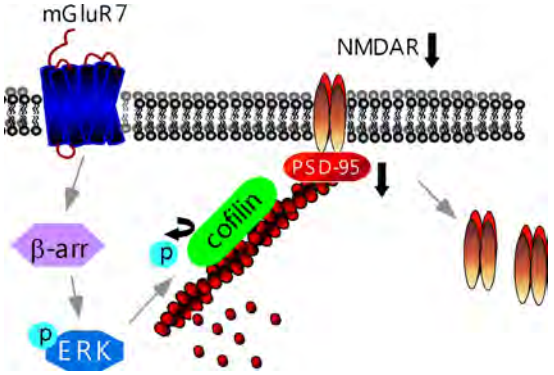


FIGURE 10. **Schematic model for mGluR7 regulation of NMDARs.** Activation of mGluR7, via the $\beta$-arrestin2 ($\beta$-*arr*)/ERK pathway, triggers the increase of cofilin activity by decreasing its phosphorylation (*P*), leading to the increased actin depolymerization. Consequently, the NR1/PSD-95/actin interactions are interfered, causing the internalization of NMDARs and the reduction of NMDA responses.

pendent mechanism, which results in the reduction of NMDAR currents.

## DISCUSSION

In this study, we have revealed the regulation of NMDA receptors by mGluR7 signaling (Fig. 10). The mGluR subtypes, which have heterogeneous distribution and differential signal transduction mechanisms, are thought to serve as a modulator to fine-tune synaptic efficacy in distinct manners (34, 52) All three groups of mGluRs have been linked to long-term synaptic plasticity such as long-term potentiation/long-term depression (53, 54). Previous slice recordings have shown that group III mGluRs could act presynaptically to reduce glutamatergic and GABAergic transmission at different synapses (36, 55–57). However, mGluR4 has been found to be expressed postsynaptically as well as presynaptically in hippocampus by anatomic studies (58). Functional studies also suggest that postsynaptic mGluR4 might mediate the reducing effect of a low concentration of L-AP4 (20 $\mu$M) on the inward current evoked by exogenous NMDA application in nucleus accumbens slices (59). The pre- and postsynaptic presence of mGluR7 (22–24) suggests that mGluR7 may have postsynaptic functions, which are masked by presynaptic actions when examining in brain slices.

Because the effects of mGluR agonists on NMDAR-EPSC in slices could be mediated by either presynaptic or postsynaptic actions, we mainly used freshly isolated neurons from slices, which have the following advantages. First, it is a pure postsynaptic system, so we are able to reveal the postsynaptic action of mGluRs. Second, NMDAR-mediated current can be measured accurately with fast application of ligand (NMDA) to the cell under recording. Third, the intracellular mechanism underlying mGluR regulation of NMDARs can be investigated directly without the indirect effects from neighboring neurons at the circuit. Using combined electrophysiological, biochemical, and immunocytochemical approaches, we have revealed an inhibitory effect on NMDAR trafficking and function by group III mGluRs in PFC pyramidal neurons. Pharmacological studies and cellular knockdown experiments indicate that mGluR7 is the receptor mediating this postsynaptic effect.

Downloaded from www.jbc.org at State University of NY-Buffalo, on March 29, 2012

Emerging evidence suggests that NMDA receptors undergo regulated transport to and from the cell surface and lateral diffusion at synaptic and extrasynaptic sites in the plasma membrane (60). NMDARs are tethered to actin cytoskeleton via scaffolding and adaptor proteins such as $\alpha$-actinin and PSD-95 (61, 62). Actin depolymerization reduces NMDA channel activity (63) and the number of synaptic NMDAR clusters (49). Moreover, actin depolymerization plays a key role in triggering long-term depression of NMDA synaptic responses in hippocampus (64). Here we provide multiple lines of evidence showing that mGluR7, via activation of ERK, increases the actin-depolymerizing activity of cofilin, leading to the loss of actin filaments at synapses. Consequently, the association of NMDARs with actin and PSD-95 is reduced, which causes the loss of surface NMDAR clusters and the depression of NMDAR currents. This mGluR7-mediated regulation of NMDA responses is different from group I mGluR-induced long-term depression, which is due to the increased AMPAR endocytosis rate (65, 66) mediated by the dendritic synthesis of Arc/Arg3.1, an activity-regulated cytoskeleton-associated protein (67).

Unlike the presynaptically located mGluRs, which inhibit transmitter release and therefore affect the response of many postsynaptic receptor subtypes, the postsynaptic modulation of NMDARs by mGluR7 offers a way for more specific regulation. Given the key role of NMDARs in cognition and emotion (25, 68), our results provide a potential mechanism for the involvement of mGluR7 in a variety of PFC-controlled mental functions, which was revealed from mGluR7 deficient mice (9, 10, 14).

*Acknowledgment—We thank Xiaoqing Chen for technical support.*

## REFERENCES


1. Nakanishi, S. (1992) Molecular diversity of glutamate receptors and implications for brain function. *Science* **258,** 597–603
2. Swanson, C. J., Bures, M., Johnson, M. P., Linden, A. M., Monn, J. A., and Schoepp, D. D. (2005) Metabotropic glutamate receptors as novel targets for anxiety and stress disorders. *Nat. Rev. Drug Discov.* **4,** 131–144
3. Lavreysen, H., and Dautzenberg, F. M. (2008) Therapeutic potential of group III metabotropic glutamate receptors. *Curr. Med. Chem.* **15,** 671–684
4. Field, J. R., Walker, A. G., and Conn, P. J. (2011) Targeting glutamate synapses in schizophrenia. *Trends Mol. Med.* **17,** 689–698
5. Helton, D. R., Tizzano, J. P., Monn, J. A., Schoepp, D. D., and Kallman, M. J. (1998) Anxiolytic and side-effect profile of LY354740: a potent, highly selective, orally active agonist for group II metabotropic glutamate receptors. *J. Pharmacol. Exp. Ther.* **284,** 651–660
6. Spooren, W. P., Vassout, A., Neijt, H. C., Kuhn, R., Gasparini, F., Roux, S., Porsolt, R. D., and Gentsch, C. (2000) Anxiolytic-like effects of the prototypical metabotropic glutamate receptor 5 antagonist 2-methyl-6-(phenylethynyl)pyridine in rodents. *J. Pharmacol. Exp. Ther.* **295,** 1267–1275
7. Pałucha, A., Tatarczyńska, E., Brański, P., Szewczyk, B., Wierońska, J. M., Kłak, K., Chojnacka-Wójcik, E., Nowak, G., and Pilc, A. (2004) Group III mGlu receptor agonists produce anxiolytic- and antidepressant-like effects after central administration in rats. *Neuropharmacology* **46,** 151–159
8. Sansig, G., Bushell, T. J., Clarke, V. R., Rozov, A., Burnashev, N., Portet, C., Gasparini, F., Schmutz, M., Klebs, K., Shigemoto, R., Flor, P. J., Kuhn, R., Knoepfel, T., Schroeder, M., Hampson, D. R., Collett, V. J., Zhang, C., Duvoisin, R. M., Collingridge, G. L., and van Der Putten, H. (2001) Increased seizure susceptibility in mice lacking metabotropic glutamate receptor 7. *J. Neurosci.* **21,** 8734–8745
9. Hölscher, C., Schmid, S., Pilz, P. K., Sansig, G., van der Putten, H., and Plappert, C. F. (2004) Lack of the metabotropic glutamate receptor subtype 7 selectively impairs short-term working memory but not long-term memory. *Behav. Brain Res.* **154,** 473–481
10. Callaerts-Vegh, Z., Beckers, T., Ball, S. M., Baeyens, F., Callaerts, P. F., Cryan, J. F., Molnar, E., and D'Hooge R. (2006) Concomitant deficits in working memory and fear extinction are functionally dissociated from reduced anxiety in metabotropic glutamate receptor 7-deficient mice. *J. Neurosci.* **26,** 6573–6582
11. Masugi, M., Yokoi, M., Shigemoto, R., Muguruma, K., Watanabe, Y., Sansig, G., van der Putten, H., and Nakanishi, S. (1999) Metabotropic glutamate receptor subtype 7 ablation causes deficit in fear response and conditioned taste aversion. *J. Neurosci.* **19,** 955–963
12. Fendt, M., Schmid, S., Thakker, D. R., Jacobson, L. H., Yamamoto, R., Mitsukawa, K., Maier, R., Natt, F., Hüsken, D., Kelly, P. H., McAllister, K. H., Hoyer, D., van der Putten, H., Cryan, J. F., and Flor, P. J. (2008) mGluR7 facilitates extinction of aversive memories and controls amygdala plasticity. *Mol. Psychiatry.* **13,** 970–979
13. Mitsukawa, K., Mombereau, C., Lötscher, E., Uzunov, D. P., van der Putten, H., Flor, P. J., and Cryan, J. F. (2006) Metabotropic glutamate receptor subtype 7 ablation causes dysregulation of the HPA axis and increases hippocampal BDNF protein levels: implications for stress-related psychiatric disorders. *Neuropsychopharmacology* **31,** 1112–1122
14. Cryan, J. F., Kelly, P. H., Neijt, H. C., Sansig, G., Flor, P. J., and van Der Putten, H. (2003) Antidepressant and anxiolytic-like effects in mice lacking the group III metabotropic glutamate receptor mGluR7. *Eur. J. Neurosci.* **17,** 2409–2417
15. Palucha, A., Klak, K., Branski, P., van der Putten, H., Flor, P. J., and Pilc, A. (2007) Activation of the mGlu7 receptor elicits antidepressant-like effects in mice. *Psychopharmacology* **194,** 555–562
16. Perroy, J., Prezeau, L., De Waard, M., Shigemoto, R., Bockaert, J., and Fagni, L. (2000) Selective blockade of P/Q-type calcium channels by the metabotropic glutamate receptor type 7 involves a phospholipase C pathway in neurons. *J. Neurosci.* **20,** 7896–7904
17. Perroy, J., El Far, O., Bertaso, F., Pin, J. P., Betz, H., Bockaert, J., and Fagni, L. (2002) PICK1 is required for the control of synaptic transmission by the metabotropic glutamate receptor 7. *EMBO J.* **21,** 2990–2999
18. Pelkey, K. A., Lavezzari, G., Racca, C., Roche, K. W., and McBain, C. J. (2005) mGluR7 is a metaplastic switch controlling bidirectional plasticity of feedforward inhibition. *Neuron* **46,** 89–102
19. Pelkey, K. A., Topolnik, L., Lacaille, J. C., and McBain, C. J. (2006) Compartmentalized $Ca^{2+}$ channel regulation at divergent mossy-fiber release sites underlies target cell-dependent plasticity. *Neuron* **52,** 497–510
20. Ohishi, H., Akazawa, C., Shigemoto, R., Nakanishi, S., and Mizuno, N. (1995) Distributions of the mRNAs for L-2-amino-4-phosphonobutyrate-sensitive metabotropic glutamate receptors, mGluR4 and mGluR7, in the rat brain. *J. Comp. Neurol.* **360,** 555–570
21. Iacovelli, L., Bruno, V., Salvatore, L., Melchiorri, D., Gradini, R., Caricasole, A., Barletta, E., De Blasi, A., and Nicoletti, F. (2002) Native group III metabotropic glutamate receptors are coupled to the mitogen-activated protein kinase/phosphatidylinositol-3-kinase pathways. *J. Neurochem.* **82,** 216–223
22. Brandstätter, J. H., Koulen, P., Kuhn, R., van der Putten, H., and Wässle, H. (1996) Compartmental localization of a metabotropic glutamate receptor (mGluR7): two different active sites at a retinal synapse. *J. Neurosci.* **16,** 4749–4756
23. Kinzie, J. M., Shinohara, M. M., van den Pol, A. N., Westbrook, G. L., and Segerson, T. P. (1997) Immunolocalization of metabotropic glutamate receptor 7 in the rat olfactory bulb. *J. Comp. Neurol.* **385,** 372–384
24. Kosinski, C. M., Risso Bradley, S., Conn, P. J., Levey, A. I., Landwehrmeyer, G. B., Penney, J. B., Jr., Young, A. B., and Standaert, D. G. (1999) Localization of metabotropic glutamate receptor 7 mRNA and mGluR7a protein in the rat basal ganglia. *J. Comp. Neurol.* **415,** 266–284
25. Tsai, G., and Coyle, J. T. (2002) Glutamatergic mechanisms in schizophrenia. *Annu. Rev. Pharmacol. Toxicol.* **42,** 165–179
26. Moghaddam, B. (2003) Bringing order to the glutamate chaos in schizophrenia. *Neuron* **40,** 881–884
27. Andreasen, N. C., O'Leary, D. S., Flaum, M., Nopoulos, P., Watkins, G. L.,


Downloaded from www.jbc.org at State University of NY-Buffalo, on March 29, 2012

Boles Ponto, L. L., and Hichwa, R. D. (1997) Hypofrontality in schizophrenia: distributed dysfunctional circuits in neuroleptic-naive patients. *Lancet* **349,** 1730–1734
28. Drevets, W. C., Ongür, D., and Price, J. L. (1998) Neuroimaging abnormalities in the subgenual prefrontal cortex: implications for the pathophysiology of familial mood disorders. *Mol. Psychiatry* **3,** 220–226, 190–191
29. Miller, E. K., and Cohen, J. D. (2001) An integrative theory of prefrontal cortex function. *Annu. Rev. Neurosci.* **24,** 167–202
30. Gu, Z., Jiang, Q., Fu, A. K., Ip, N. Y., and Yan, Z. (2005) Regulation of NMDA receptors by neuregulin signaling in prefrontal cortex. *J. Neurosci.* **25,** 4974–4984
31. Yuen, E. Y., Liu, W., Karatsoreos, I. N., Feng, J., McEwen, B. S., and Yan, Z. (2009) Acute stress enhances glutamatergic transmission in prefrontal cortex and facilitates working memory. *Proc. Natl. Acad. Sci. U.S.A.* **106,** 14075–14079
32. Yuen, E. Y., Jiang, Q., Chen, P., Gu, Z., Feng, J., and Yan, Z. (2005) Serotonin 5-HT1A receptors regulate NMDA receptor channels through a microtubule-dependent mechanism. *J. Neurosci.* **25,** 5488–5501
33. Wang, X., Zhong, P., Gu, Z., and Yan, Z. (2003) Regulation of NMDA receptors by dopamine D4 signaling in prefrontal cortex. *J. Neurosci.* **23,** 9852–9861
34. Conn, P. J., and Pin, J. P. (1997) Pharmacology and functions of metabotropic glutamate receptors. *Annu. Rev. Pharmacol. Toxicol.* **37,** 205–237
35. Schoepp, D. D., Jane, D. E., and Monn, J. A. (1999) Pharmacological agents acting at subtypes of metabotropic glutamate receptors. *Neuropharmacology* **38,** 1431–1476
36. Gereau, R. W., 4th, and Conn, P. J. (1995) Multiple presynaptic metabotropic glutamate receptors modulate excitatory and inhibitory synaptic transmission in hippocampal area CA1. *J. Neurosci.* **15,** 6879–6889
37. Martín, R., Torres, M., and Sánchez-Prieto, J. (2007) mGluR7 inhibits glutamate release through a PKC-independent decrease in the activity of P/Q-type $Ca^{2+}$ channels and by diminishing cAMP in hippocampal nerve terminals. *Eur. J. Neurosci.* **26,** 312–322
38. Ayala, J. E., Niswender, C. M., Luo, Q., Banko, J. L., and Conn, P. J. (2008) Group III mGluR regulation of synaptic transmission at the SC-CA1 synapse is developmentally regulated. *Neuropharmacology* **54,** 804–814
39. Okamoto, N., Hori, S., Akazawa, C., Hayashi, Y., Shigemoto, R., Mizuno, N., and Nakanishi, S. (1994) Molecular characterization of a new metabotropic glutamate receptor mGluR7 coupled to inhibitory cyclic AMP signal transduction. *J. Biol. Chem.* **269,** 1231–1236
40. Luttrell, L. M., Ferguson, S. S., Daaka, Y., Miller, W. E., Maudsley, S., Della Rocca, G. J., Lin, F., Kawakatsu, H., Owada, K., Luttrell, D. K., Caron, M. G., and Lefkowitz, R. J. (1999) $\beta$-Arrestin-dependent formation of $\beta$2 adrenergic receptor-Src protein kinase complexes. *Science* **283,** 655–661
41. Lefkowitz, R. J., and Shenoy, S. K. (2005) Transduction of receptor signals by $\beta$-arrestins. *Science* **308,** 512–517
42. Jiang, Q., Yan, Z., and Feng, J. (2006) Activation of group III metabotropic glutamate receptors attenuates rotenone toxicity on dopaminergic neurons through a microtubule-dependent mechanism. *J. Neurosci.* **26,** 4318–4328
43. dos Remedios, C. G., Chhabra, D., Kekic, M., Dedova, I. V., Tsubakihara, M., Berry, D. A., and Nosworthy, N. J. (2003) Actin-binding proteins: regulation of cytoskeletal microfilaments. *Physiol. Rev.* **83,** 433–473
44. Morgan, T. E., Lockerbie, R. O., Minamide, L. S., Browning, M. D., and Bamburg, J. R. (1993) Isolation and characterization of a regulated form of actin-depolymerizing factor. *J. Cell Biol.* **122,** 623–633
45. Pawlak, G., and Helfman, D. M. (2002) MEK mediates v-Src-induced disruption of the actin cytoskeleton via inactivation of the Rho-ROCK-LIM kinase pathway. *J. Biol. Chem.* **277,** 26927–26933
46. Nebl, G., Fischer, S., Penzel, R., and Samstag, Y. (2004) Dephosphorylation of cofilin is regulated through Ras and requires the combined activities of the Ras effectors MEK and PI3K. *Cell. Signal.* **16,** 235–243
47. Aizawa, H., Wakatsuki, S., Ishii, A., Moriyama, K., Sasaki, Y., Ohashi, K., Sekine-Aizawa, Y., Sehara-Fujisawa, A., Mizuno, K., Goshima Y., and Yahara, I. (2001) Phosphorylation of cofilin by LIM kinase is necessary for semaphorin 3A-induced growth cone collapse. *Nat. Neurosci.* **4,** 367–373
48. Zhou, Q., Homma, K. J., and Poo, M. M. (2004) Shrinkage of dendritic spines associated with long-term depression of hippocampal synapses. *Neuron* **44,** 749–757
49. Allison, D. W., Gelfand, V. I., Spector, I., and Craig, A. M. (1998) Role of actin in anchoring postsynaptic receptors in cultured hippocampal neurons: differential attachment of NMDA versus AMPA receptors. *J. Neurosci.* **18,** 2423–2436
50. Roche, K. W., Standley, S., McCallum, J., Dune Ly, C., Ehlers, M. D., and Wenthold, R. J. (2001) Molecular determinants of NMDA receptor internalization. *Nat. Neurosci.* **4,** 794–802
51. Lin, Y., Skeberdis, V. A., Francesconi, A., Bennett, M. V., and Zukin, R. S. (2004) Postsynaptic density protein-95 regulates NMDA channel gating and surface expression. *J. Neurosci.* **24,** 10138–10148
52. Schoepp, D. D., and Conn, P. J. (1993) Metabotropic glutamate receptors in brain function and pathology. *Trends Pharmacol. Sci.* **14,** 13–20
53. Anwyl, R. (1999) Metabotropic glutamate receptors: electrophysiological properties and role in plasticity. *Brain Res. Brain Res. Rev.* **29,** 83–120
54. Bellone, C., Lüscher, C., and Mameli, M. (2008) Mechanisms of synaptic depression triggered by metabotropic glutamate receptors. *Cell. Mol. Life Sci.* **65,** 2913–2923
55. Salt, T. E., and Eaton, S. A. (1995) Distinct presynaptic metabotropic receptors for L-AP4 and CCG1 on GABAergic terminals: pharmacological evidence using novel $\alpha$-methyl derivative mGluR antagonists, MAP4 and MCCG, in the rat thalamus *in vivo*. *Neuroscience* **65,** 5–13
56. Bushell, T. J., Jane, D. E., Tse, H. W., Watkins, J. C., Garthwaite, J., and Collingridge, G. L. (1996) Pharmacological antagonism of the actions of group II and III mGluR agonists in the lateral perforant path of rat hippocampal slices. *Br. J. Pharmacol.* **117,** 1457–1462
57. Pisani, A., Calabresi, P., Centonze, D., and Bernardi, G. (1997) Activation of group III metabotropic glutamate receptors depresses glutamatergic transmission at corticostriatal synapse. *Neuropharmacology* **36,** 845–851
58. Bradley, S. R., Levey, A. I., Hersch, S. M., and Conn, P. J. (1996) Immunocytochemical localization of group III metabotropic glutamate receptors in the hippocampus with subtype-specific antibodies. *J. Neurosci.* **16,** 2044–2056
59. Martin, G., Nie, Z., and Siggins, G. R. (1997) Metabotropic glutamate receptors regulate *N*-methyl-D-aspartate-mediated synaptic transmission in nucleus accumbens. *J. Neurophysiol.* **78,** 3028–3038
60. Wenthold, R. J., Prybylowski, K., Standley, S., Sans, N., and Petralia, R. S. (2003) Trafficking of NMDA receptors. *Annu. Rev. Pharmacol. Toxicol.* **43,** 335–358
61. Wyszynski, M., Lin, J., Rao, A., Nigh, E., Beggs, A. H., Craig, A. M., and Sheng, M. (1997) Competitive binding of $\alpha$-actinin and calmodulin to the NMDA receptor. *Nature* **385,** 439–442
62. Pak, D. T., Yang, S., Rudolph-Correia, S., Kim, E., and Sheng, M. (2001) Regulation of dendritic spine morphology by SPAR, a PSD-95-associated RapGAP. *Neuron* **31,** 289–303
63. Rosenmund, C., and Westbrook, G. L. (1993) Calcium-induced actin depolymerization reduces NMDA channel activity. *Neuron* **10,** 805–814
64. Morishita, W., Marie, H., and Malenka, R. C. (2005) Distinct triggering and expression mechanisms underlie LTD of AMPA and NMDA synaptic responses. *Nat. Neurosci.* **8,** 1043–1050
65. Snyder, E. M., Philpot, B. D., Huber, K. M., Dong, X., Fallon, J. R., and Bear, M. F. (2001) Internalization of ionotropic glutamate receptors in response to mGluR activation. *Nat. Neurosci.* **4,** 1079–1085
66. Huang, C. C., You, J. L., Wu, M. Y., and Hsu, K. S. (2004) Rap1-induced p38 mitogen-activated protein kinase activation facilitates AMPA receptor trafficking via the GDI·Rab5 complex: potential role in (*S*)-3,5-dihydroxyphenylglycene-induced long-term depression. *J. Biol. Chem.* **279,** 12286–12292
67. Waung, M. W., Pfeiffer, B. E., Nosyreva, E. D., Ronesi, J. A., and Huber, K. M. (2008) Rapid translation of Arc/Arg3.1 selectively mediates mGluR-dependent LTD through persistent increases in AMPAR endocytosis rate. *Neuron* **59,** 84–97
68. Lisman, J. E., Fellous, J. M., and Wang, X. J. (1998) A role for NMDA-receptor channels in working memory. *Nat. Neurosci.* **1,** 273–275

Downloaded from www.jbc.org at State University of NY-Buffalo, on March 29, 2012